The MU radar with an active phased array system
2. In-house equipment

Shoichiro Fukao,[1,2] *Toshitaka Tsuda,*[3] *Toru Sato,*[3] *Susumu Kato,*[3] *Koichiro Wakasugi,*[4]
and Tsuneichi Makihira[5]

Reprinted from
RADIO SCIENCE
Volume 20 Number 6 November/December 1985

Radio Science, Volume 20, Number 6, Pages 1169–1176, November–December 1985

The MU radar with an active phased array system
2. In-house equipment

Shoichiro Fukao,[1,2] *Toshitaka Tsuda,*[3] *Toru Sato,*[3] *Susumu Kato,*[3] *Koichiro Wakasugi,*[4] *and Tsuneichi Makihira*[5]

(Received February 14, 1985; revised June 11, 1985; accepted June 26, 1985.)

The MU (middle and upper atmosphere) radar of Japan uses an active phased array system. Each of 475 crossed three-subelement yagi antennas in a circular array is provided with a 2.4-kW peak power amplifier. This system configuration attains a very fast and almost continuous beam steerability at the total peak radiation power of 1 MW. A brief description of the in-house equipment is presented herein.

1. INTRODUCTION

The middle and upper atmosphere (MU) radar, Shigaraki, Shiga, Japan (34.85°N, 136.10°E), is the first mesosphere-stratosphere-troposphere (MST) radar that can steer the antenna beam fast and almost continuously. This capability originates from its unique system configuration.

The conventional radars employ a passive phased array connected to a high-power transmitter [e.g., *Green et al.*, 1979; *Schmidt et al.*, 1979; *Czechowsky et al.*, 1984L. In the MU radar array, each antenna element is fed by a low-power amplifier, and all amplifiers are coherently driven to radiate 1-MW peak output power. Because phase shift and signal division/combination are conducted at low signal levels, fast and almost continuous beam steering, as well as various sophisticated operations, employing several independent beams, are made feasible. For the same reason, the entire system can be easily controlled with the aid of a computer.

The system outline of the MU radar along with a few preliminary results have been presented by *Kato et al.* [1984], and details of the antenna and transmitters are described by *Fukao et al.* [this issue] (hereafter referred to as paper 1). The present paper mainly describes the in-house equipment related to transmission, reception, on-line data processing and system control.

2. TRANSMISSION AND RECEPTION

2.1. *Reference analog and timing signals*

Various analog signals required for transmission (TX) and reception (RX) and timing signals for system control are generated by a combination of a Rubidium-vapor master oscillator, a frequency synthesizer and a timing signal generator as shown in Figure 1. The intermediate frequency (IF) signal of 5 MHz used for transmission and detection, and the local frequency signal of 41.5 MHz are synthesized from the reference signals of 1 and 5 MHz. The frequency synthesizer also generates the reference digital clock of 4 MHz. The 4-MHz clock is utilized in the timing signal generator where various timing signals required for real time system control are generated according to instructions from the radar controller.

Some details of the control data set by the radar controller are as follows. The MU radar starts/stops its operation by means of TX start/stop control data. The number of subpulses is indicated when pulse compression is conducted. In the case that transmission of multiple pulses [*Farley*, 1972] (up to seven pulses) is incorporated, a TX pulse sequence and the total length of this sequence are set. The RX gate is opened at a preset time to begin signal sampling. Sampling ends when the desired number of samples have been taken. The coherent-integration-end signal is generated when transmission and reception are repeated the number of times needed for coherent integration. Sampling start timing can be changed by a

[1]Department of Electrical Engineering, Kyoto University, Yoshida, Japan.
[2]Now at Radio Atmospheric Science Center, Kyoto University.
[3]Radio Atmospheric Science Center, Kyoto University, Uji, Japan.
[4]Department of Electrical Engineering, Kyoto Institute of Technology, Matsugasaki, Japan.
[5]Communication Equipment Works, Mitsubishi Electric Corporation, Amagasaki, Hyogo, Japan.

Paper number 5S0524.
0048-6604/85/005S-0524$08.00

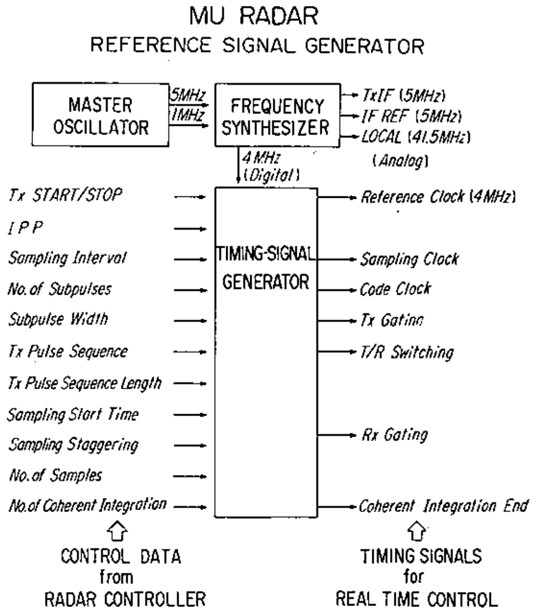

Fig. 1. Block diagram of the reference signal generator. Control data are set by the radar controller. Timing signals are sent to various system hardware for real time control.

half or quarter of the sampling interval in order to stagger range gates within a scattering volume. Other control data and timing signals are referred to in Figure 1.

2.2. *Transmission*

The 5-MHz TX IF signal is modulated to provide coded pulses by the modulator as shown in Figure 2. The binary code for pulse compression is loaded by T/R switching signal into the shift register of the code generator unit. At the instant that the TX gate is opened, the code is sent to the modulator unit. The TX IF signal is then pulse-modulated by this code. The linear phase low-pass filter (seven-stage Thomson type) is switched to match subpulse widths of 1, 2, 4, 8, 16 and 32 μs. The phase of the code can be flipped 180° after every two pulses in order to eliminate any system offset. Any kind of binary code with a length of up to 32 elements is applicable. At present, 16- or 32-element complementary codes [e.g., *Schmidt et al.*, 1979; *Wakasugi and Fukao*, 1985] are being used for observation of the middle atmosphere, whereas a 7- or 13-element Barker code [*Gray and Farley*, 1973] is employed for observation of the ionosphere. A typical seven-element Barker coded pulse with 1-μs subpulse width is illustrated in Figure 3.

The modulated TX IF signal is sent to the divider and split into 6, each segment being sent to a remote booth accommodating transmitter-receiver (TR) modules. The local signal and T/R switching signal are also split at the divider and sent to each booth. Both the upconvert to RF (46.5 MHz) and power amplification are made in the TR modules (paper 1). As shown in the standard level diagram (Figure 4), the signal levels of both IF and local are approximately 0 dBm up to the output port of the divider.

Attenuation is provided in the modulator unit for CW transmission at reduced total radiation power of 50–400 W.

2.3. *Reception*

The received 46.5-MHz signal is first amplified by the preamplifier and then downconverted to IF at the mixer (MIX) unit in the TR modules (paper 1). The IF signals from the 19 modules in each group are then combined into one and sent to combiner in the control building. The IF signals from all 25 groups are combined into one to four channels in any combination. Only one channel is used for normal full power operation. The IF signals are amplified by a 60-dB gain stage to an optimum input level for the detector (Figure 5).

Four coherent detectors are available, corresponding to the four output channels of the combiner. The

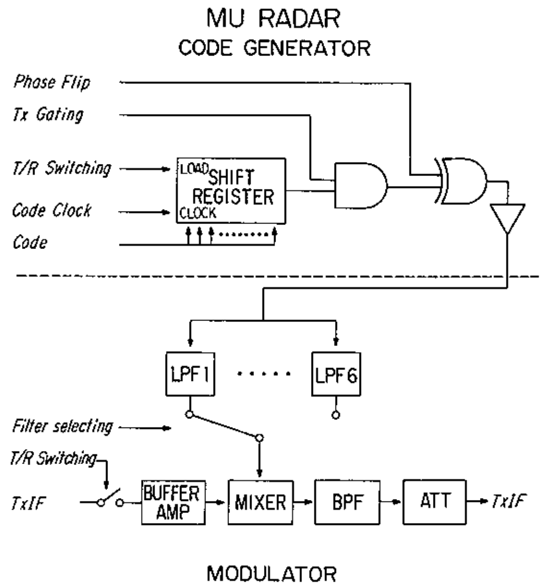

Fig. 2. Block diagram of the modulator. The pulse compression signal generated at the code generator unit is sent to the modulator unit to phase-code the 5-MHz TX IF signal.

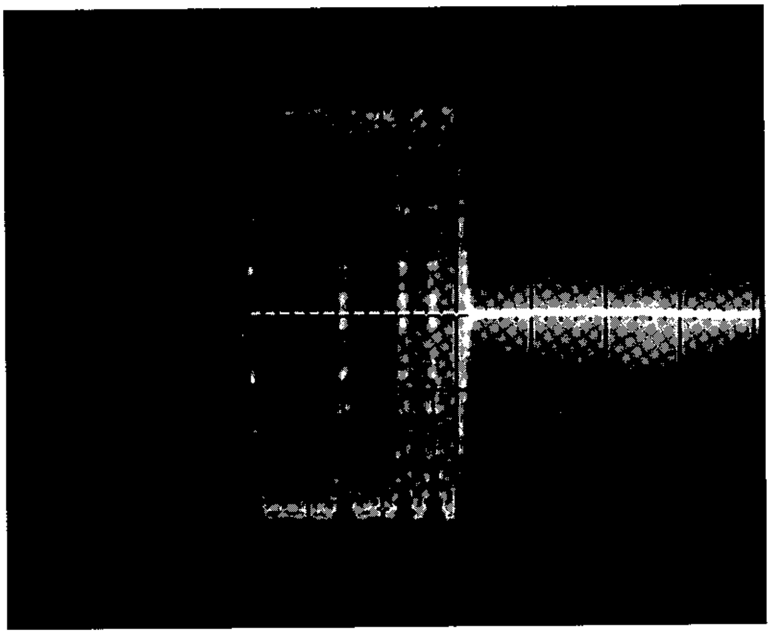

Fig. 3. TX IF pulse modulated by a seven-element Barker code with a subpulse width of 1 μs.

IF signal is split and separately mixed with two phase-quadrature reference signals (5 MHz). This detection enables determination of the sign of the Doppler-shifted echo. The same low-pass filter as is used for the modulator is provided in each detector channel to match TX subpulse widths of 1, 2, 4, 8, 16 and 32 μs. The video amplifier in each channel matches the filtered signal to the desired input level of the analog-to-digital (A/D) converters in the demodulator/integrator.

Twelve-bit digitized signals are decoded for pulse compression and then coherently integrated, as illustrated in Figure 6. Coherent integration prior to decoding is possible only when the characteristic time of atmospheric refractive-index fluctuations is much larger than the period required for coherent integration [*Schmidt et al.*, 1979; *Woodman et al.*, 1980]. Since the MU radar incorporates pulse compression also for the purpose of observing the ionosphere with a characteristic time less than interpulse periods (IPP), decoding prior to/without coherent integration is required.

Figure 7 shows the decoding scheme of the MU radar. Decoding demands cross correlation of *Ci* and

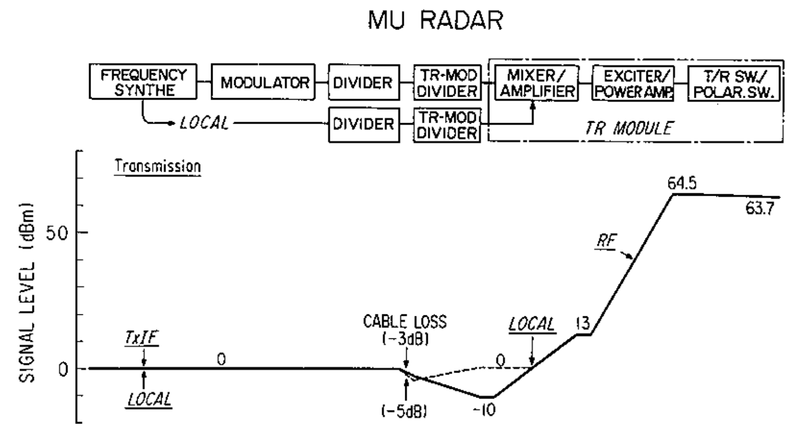

Fig. 4. Standard level diagram for transmission. The final output power of 63.7 dBm is provided for linear polarizations. The signal level at a few stages is given in units of decibels referred to 1 mW.

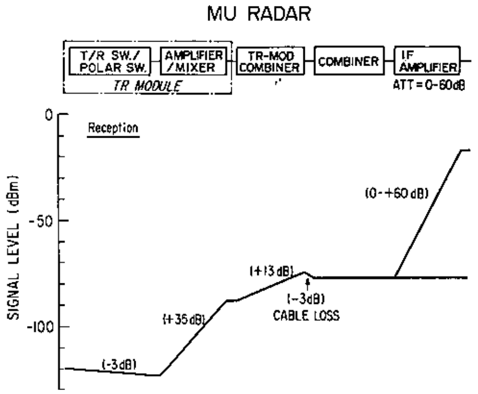

Fig. 5. Standard level diagram for reception of an input signal of −120 dBm.

Ri, where Ci and Ri are the transmitted code and the received M bit digital signal of sine/cosine channels, respectively. As Ri is expressed in the following form,

$$Ri = \sum_{k=0}^{M-1} R_i^k 2^k$$

the decoded signal $\overline{Ri}$ is given by

$$\begin{aligned}\overline{Ri} &= \sum_{j=1}^{N} CjR_{i+j} \\ &= \left(\sum_{j=1}^{N} CjR_{i+j}^0\right)2^0 + \left(\sum_{j=1}^{N} CjR_{i+j}^1\right)2^1 + \cdots \\ &+ \left(\sum_{j=1}^{N} CjR_{i+j}^{M-1}\right)2^{M-1} \end{aligned} \quad (1)$$

where N is the code length. The diagram indicates that the convolution is taken at each bit of consecutive data and that summation is performed in a pipeline operation as shown in (1). Because Ri is either 1 or 0 and Ci is either $+1$ or -1, implementation of the decoder hardware is significantly simplified. This makes it possible to decode the compressed pulse in real time, a capability which is essential to ionosphere observations.

The coherent integrator consists of two memories of 1024-word length for 1024 complex samples, one for each of the phase quadrature data (Figure 6). They are switched alternately to their integration or reading-out modes. Coherent integration is allowed up to 256 times. The integrated data are sent to the buffer memory of the array processor for on-line processing.

3. ON-LINE DATA PROCESSING

The method of processing the coherently integrated, digitized data is schematically shown in Figure 8. The main constituents of the system are a host computer VAX-11/750 (hereafter referred to as VAX) and an array processor MAP-300 (MAP). Fast Fourier transform (FFT) or autocorrelation function (ACF) are calculated in real time by MAP under the supervision of VAX. A 2-Mbyte random access memory (2-MB RAM) of the MAP is used as two concurrently operating buffer memories. One is the input buffer, to which coherently integrated phase quadrature data are sent. The other is the incoherent integration buffer, where power spectra under incoherent integration are temporarily stored.

The on-line processing data flow is schematically shown in the same figure. When the desired number of data are stored in the input buffer, MAP resets ISPL (initial set pulse) to momentarily interrupt TX. During this period MAP reads out the data in order to calculate power spectra by means of an FFT algo-

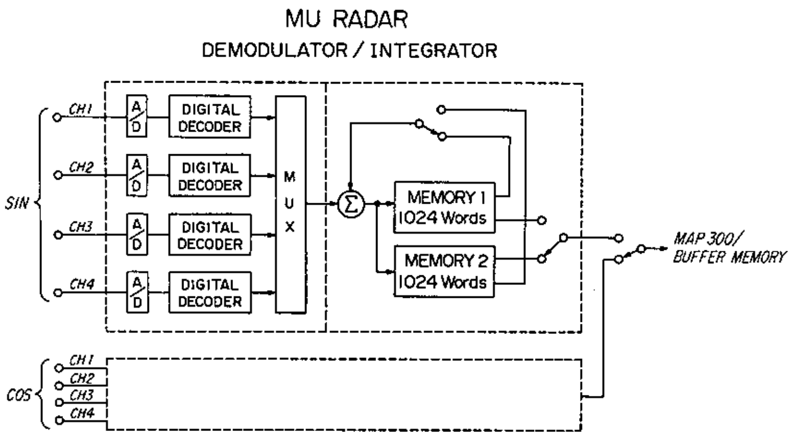

Fig. 6. Block diagram of the demodulator/integrator. Two phase quadrature signals from each detector channel have their own analog-to-digital (A/D) converters of 1 MHz. MUX indicates a multiplexer.

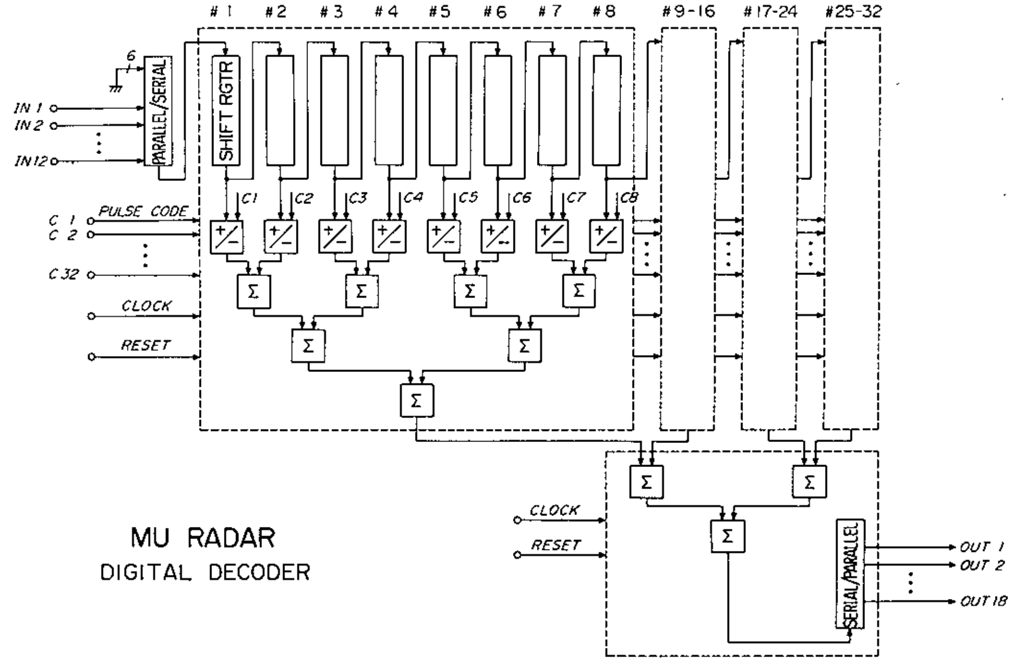

Fig. 7. A detailed block diagram of the digital decoder for pulse compression. Six dummy bits are added to the input data to allow conformance up to 32 summations. The serial-to-parallel conversion is actually performed in the MUX shown in Figure 6.

rithm. The calculated results are added to the power spectrum sums read out of the incoherent integration buffer. Then MAP sets ISPL to restart TX. This pause occupies no more than a few percent of the total observational time for standard lower stratosphere observations. After incoherent integration has been repeated a preset number of times, the power spectra are transferred to VAX via MAP and stored in the magnetic disk. The data are then read out from the disk files and recorded on magnetic tape (MT). The disk files form a ring buffer storing the 10 most recent pieces of data. These data are immediately available to the operator on a color graphic display, Quick Display, if requested during observation.

The software for the on-line data processing is composed of the following three programs (processes), i.e., control program, data handling program, and Quick Display program. The data handling program controls MAP so as to calculate power spectra (or ACF's) and to write them in the ring buffer. The control program manages a package of data handling programs and executes individually according to instructions from the radar controller. It is also responsible for transferring data from the ring buffer to MT. Immediate access to the data stored in the ring buffer is provided by the Quick Display program.

It can be assumed that this software structure, with interprocess communications, is much more efficient than a single general purpose program. Such a program would be too lengthy and lack the versatility to be applicable to a variety of observations. Within the MU radar software, only the data handling programs are specially designed to handle the various types of observations; FFT, ACF, power profile mode, etc. Generally speaking, this design principle facilitates development of optimum programs with the fastest possible processing speeds. Also, data transfer from

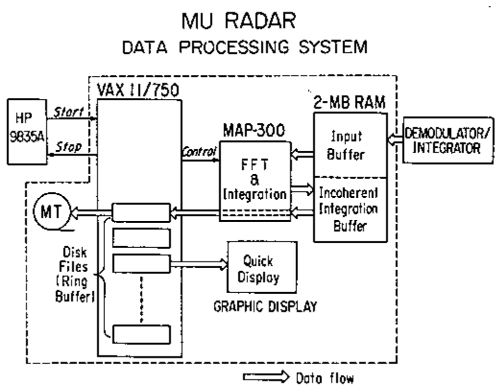

Fig. 8. Principal constituents for on-line data processing (inside the dotted square). Data flow is indicated by thick arrows. The magnetic disk is shown inclusive in VAX because, from a software point of view, it belongs to VAX.

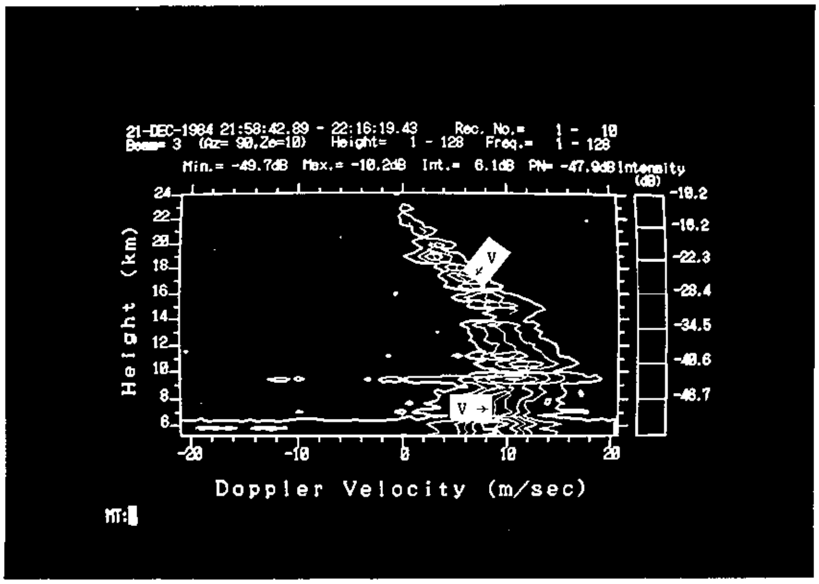

Fig. 9. A sample of the on-line graphic display of Doppler spectra obtained in the vertical direction at 128 heights in a range of 5.4–24.5 km. Contours of the Doppler spectra are shown in terms of the equivalent radial velocity. The thin (dotted) line indicated by V shows the mean Doppler shift inferred by a nonlinear fitting of Gaussian function in real time.

the disk to MT, a comparatively slow process, is not conducted by the data handling program but by the control program, obviating any loss of observation time.

The VAX performs nonlinear fitting of Gaussian functions to the observed turbulent scatter spectra to infer the mean Doppler shift in real time without any loss in data handling time. A typical example of the on-line graphic display output appears in Figure 9.

4. SYSTEM CONTROL

The MU radar system is virtually under full supervision of the radar controller. Its main constituent is a desktop computer HP9835A. The system control programs and various observational parameters are stored in a magnetic disk and read out for use in each observation.

Communication between the radar controller and system hardware is performed via both a 16-bit parallel I/O interface and RS-232C serial I/O interface. The parallel I/O is employed for control of the in-house hardware, i.e., the reference signal generator, modulator/demodulator, divider/combiner, detector and 2-MB RAM, while the serial I/O's are used for communication with VAX and the TR module controllers in the remote booths (paper 1). The transfer speed is 1200 baud.

The control and communication items are listed in Table 1, indicating the sophisticated architecture of the system control. The radar controller sends the control data concerned with transmission, reception, and data processing to the in-house equipment. The control data for the antenna are transferred to the 25 TR module controllers. During observation, the radar controller polls the TR-module controllers for monitor data from the TR modules. As mentioned above, the radar controller supervises the programs on VAX and transfers the observational parameters and name of the assigned data handling program to VAX.

The radar controller allocates the memories of the coherent integrator and the 2-MB RAM for different beams and RX channels, according to the number of FFT points, coherent integration times, and antenna beam steering mode being employed. The staggered sampling within a scattering volume is treated to appear as different beam directions in the memories. Twenty different methods of memory allocation are now feasible. Three beam modes are possible, i.e., fixed, steering every IPP (or every two IPP's), or steering after each FFT calculation. Due to hardware limitations in allocating the memories, the number of available beams is limited to 16 when both beam steering of every IPP and coherent integration are

TABLE 1. Radar Controller: Main Control and Communication Items

Hardware	Items
In-house equipment (other than the data processing system)	TX signal control
	subpulse width
	modulator filter
	pulse compression code
	TX pulse sequence
	TX IF attenuation
	IPP
	phase flip
	RX signal control
	sampling start time
	sampling interval
	number of samples
	sampling staggering
	RX channel control
	channel grouping
	RX filter
	RX IF attenuation
	data processing control
	number of coherent integrations
	memory allocation for coherent integrator and 2-MB RAM
	number of FFT/ACF points
Data processing system	data handling programs
	observational parameters
	start/stop times
TR module	activation of TR modules
	antenna
	grouping
	beam direction
	polarization
	monitor data
	TX/RX amplitude and phase
	alarms
	power supply
	fan

conducted. Otherwise, 255 beam directions are allowed.

Because the start/stop of any observation is executed with reference to the clock in VAX, the radar controller instructs VAX of the start/stop time to be used. Switchover to the different observational parameters stored in the radar controller disk can be performed automatically within a couple of minutes at scheduled times for successive observations.

5. PRELIMINARY RESULTS AND CONCLUDING REMARKS

In order to demonstrate that the MU radar functions properly, the radar-deduced winds are com-

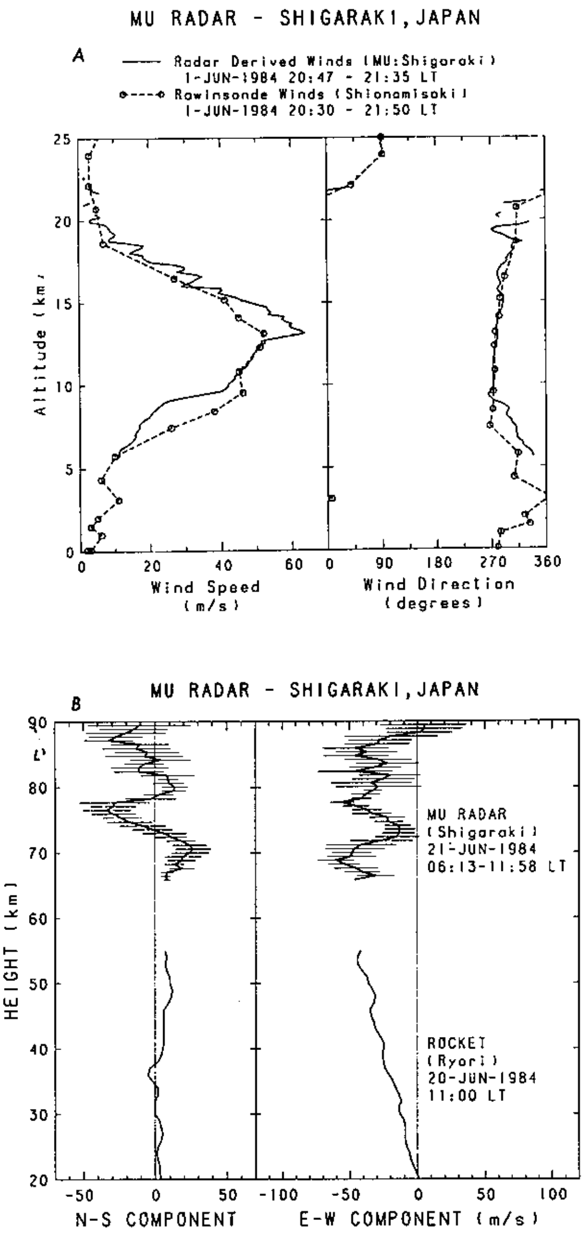

Fig. 10. (*a*) Comparison of winds between the MU radar (solid line) and the rawinsonde launched by the Japan Meteorological Agency (JMA) from Shionomisaki (dotted line with circles) on June 1, 1984. The wind speed and direction are given following meteorological conventions. The MU radar operates with 19 subarrays. The MU radar wind velocity is averaged over a period while the rawinsonde stays in the height range observed. (*b*) Comparison of winds between the MU radar (thick line with horizontal bars) and a JMA routine rocket sounding at Ryori (thin line). The MU radar winds are averaged over 0613–1158 LT on June 21, 1984. The horizontal bars show wind variation around the averaged value. The observation day of the rocket differs by 1 day as indicated in the figure.

pared with the results of observations using conventional meteorological methods. These observations are conducted by using the 19 hexagonal subarrays shown in Figure 3 of paper 1. The antenna beam is steered every IPP sequentially in three different directions, i.e., the zenith and 10° off from the zenith toward the north and east.

Figure 10*a* compares a MU radar wind profile in a height range of 5.4–24.5 km with that of a routine rawinsonde launched by the Japan Meteorological Agency (JMA) from Shionomisaki, approximately 150 km south of Shigaraki. The westerly (eastward wind) is predominant throughout this height range. The general agreement seems to be excellent between the two, considering the distance between the two observational sites.

In Figure 10*b*, the meridional and zonal wind velocities obtained in a height range of 67–90 km are compared with the meteorological rocket sounding obtained by the JMA at Ryori, about 700 km to the northeast. Although the two data patterns do not overlap, the two profiles are likely to be continuous from 60 to 70 km.

The final detailed examination of the functioning of the various equipment is currently in progress. Short-term preliminary observations are also being conducted, early results of which show that the MU radar is living up to the high standards of performance specified by the design. Some of these results are presented by *Sato et al.* [this issue], by *Wakasugi et al.* [this issue], and by *Tsuda et al.* [this issue]. The system will begin nearly continuous operations in the near future. It is expected that the MU radar, being the first in the Asian sector, will reveal interesting features of winds, waves, and turbulence in the troposphere, lower stratosphere, and some regions of the mesosphere and the ionosphere in this part of the world.

Acknowledgments. The authors are indebted to the staff of the Radio Atmospheric Science Center and Department of Electrical Engineering, Kyoto University, for their helpful support. Thanks are also due to W. E. Gordon, Rice University, Houston, Texas, for his suggestions and continuous encouragement. The MU radar is operated by the Radio Atmospheric Science Center of Kyoto University.

REFERENCES

Czechowsky, P., G. Schmidt, and R. Rüster, The mobile SOUSY Doppler radar: Technical design and first measurements, *Radio Sci.*, *19*, 441–450, 1984.

Farley, D. T., Multiple-pulse incoherent-scatter correlation function measurements, *Radio Sci.*, *7*, 661–666, 1972.

Fukao, S., T. Sato, T. Tsuda, S. Kato, K. Wakasugi, and T. Makihira, The MU radar with an active phased array system, 1, Antenna and power amplifiers, *Radio Sci.*, this issue.

Gray, R. W., and D. T. Farley, Theory of incoherent-scatter measurements using compressed pulses, *Radio Sci.*, *8*, 123–131, 1973.

Green, J. L., K. S. Gage, and T. E. VanZandt, Atmospheric measurements by VHF pulsed Doppler radar, *IEEE Trans. Geosci. Electron.*, *GE-17*, 262–280, 1979.

Kato, S., T. Ogawa, T. Tsuda, T. Sato, I. Kimura, and S. Fukao, The middle and upper atmosphere radar: First results using a partial system, *Radio Sci.*, *19*, 1475–1484, 1984.

Sato, T., T. Tsuda, S. Kato, S. Morimoto, S. Fukao, and I. Kimura, High-resolution MST observations of turbulence using the MU radar, *Radio Sci.*, this issue.

Schmidt, G., R. Rüster, and P. Czechowsky, Complementary code and digital filtering for detection of weak VHF radar signals from the mesosphere, *IEEE Trans. Geosci. Electron.*, *GE-17*, 154–161, 1979.

Tsuda, T., M. Yamamoto, T. Sato, S. Kato, and S. Fukao, Comparison observations between the MU radar and the Kyoto meteor radar, *Radio Sci.*, this issue.

Wakasugi, K., and S. Fukao, Sidelobe properties of a complementary code used in MST radar observation, *IEEE Trans. Geosci. Remote Sens.*, *GE-23*, 57–59, 1985.

Wakasugi, K., S. Fukao, S. Kato, A. Mizutani, and M. Matsuo, Air and precipitation particle motions within a cold front measured by the MU VHF radar, *Radio Sci.*, this issue.

Woodman, R. F., R. P. Kugel, and J. Röttger, A coherent integrator-decoder preprocessor for the SOUSY-VHF radar, *Radio Sci.*, *15*, 233–242, 1980.

S. Fukao, Department of Electrical Engineering, Kyoto University, Yoshida, Kyoto 606, Japan.

S. Kato, T. Sato, and T. Tsuda, Radio Atmospheric Science Center, Kyoto University, Uji, Kyoto 611, Japan.

T. Makihira, Communication Equipment Works, Mitsubishi Electric Corporation, Amagasaki, Hyogo 661, Japan.

K. Wakasugi, Department of Electrical Engineering, Kyoto Institute of Technology, Matsugasaki, Kyoto 606, Japan.